

Pressure induced reentrant electronic and magnetic state in $\text{Pr}_{0.7}\text{Ca}_{0.3}\text{MnO}_3$ manganite

Congwu Cui and Trevor A. Tyson

Physics Department, New Jersey Institute of Technology, Newark, New Jersey 07102

(Dated: received 10 June 2003)

In $\text{Pr}_{0.7}\text{Ca}_{0.3}\text{MnO}_3$, pressure induces reentrant magnetic and electronic state changes in the range 1 atm to ~ 6 GPa. The metal-insulator and magnetic transition temperatures coincide from ~ 1 to 5 GPa, decouple outside of this range and do not change monotonically with pressure. The effects may be explained by pressure tuned competition between double exchange and super exchange. The insulating state induced by pressure above ~ 5 GPa is possibly ferromagnetic, different from the ferromagnetic and antiferromagnetic phase-separated insulating state below ~ 0.8 GPa.

PACS numbers: 62.50.+p, 71.27.+a, 71.30.+h, 75.47.Lx

The colossal magnetoresistive manganite $\text{Pr}_{1-x}\text{Ca}_x\text{MnO}_3$ is a narrow bandwidth system due to the large mismatch between the Pr/Ca and Mn ion sizes. In $\text{Pr}_{1-x}\text{Ca}_x\text{MnO}_3$, it has been found that magnetic fields,^{1,2} high electric fields,³ irradiation with x-rays,^{4,5} electrons,⁶ or visible light^{7,8} can all destroy the charge ordered (CO) state and lead to a ferromagnetic (FM) conducting state with a very large resistivity drop. In compounds with a CO state, the lattice is strongly coupled with spin and charge.⁹ When the ionic charges are ordered, local distortion changes from dynamic Jahn-Teller distortion (JTD) to collective static distortions⁹ and the MnO_6 octahedra buckle.¹⁰ When the charge ordered insulating (COI) state is destroyed, a dramatic change in magnetic property and lattice structure occurs.¹¹

Under pressure, because of the bandwidth W increase, the CO state can be destroyed, and therefore a metallic state is induced. Moritomo *et al.*¹² reported that pressure (≤ 0.8 GPa) suppresses the CO state of the compound $x = 0.35, 0.4, 0.5$ and dT_{CO}/dP increases with x . In the $x = 0.3$ compound, pressure above 0.5 GPa induce a metallic transition which is described as a COI to ferromagnetic metallic (FMM) transition. Magnetic fields were found to be almost equivalent to pressure at least up to 1.5 GPa and can be scaled to pressure.

Because of the strong coupling between charge, spin and lattice in manganites, the investigation on the electronic and magnetic properties tuned by pressure induced lattice changes will contribute to understanding this complicated system and provide information for possible applications. At present, most of the high pressure studies on manganites were focused on the metal-insulator transition and carried out below ~ 2 GPa. In this range, it was found that the FM state and metallic state are coupled, which can be explained qualitatively by double exchange (DE) theory.^{12,13} It is generally believed that the application of hydrostatic pressure enhances the hopping integral t_0 and leads to a systematic increase of the Curie temperature.

$\text{Pr}_{0.7}\text{Ca}_{0.3}\text{MnO}_3$ is charge ordered below ~ 220 K, and is antiferromagnetic (AFM) and ferromagnetic phase-separated at low temperatures with $T_N \sim 130$ K and $T_C \sim 115$ K.¹⁴ When an external pressure is applied, the

low temperature COI state is destroyed and a FMM state is induced.^{12,15} By considering our results at much higher pressures (up to ~ 6.3 GPa) and other groups' results at low pressures, it was found that pressure affects the magnetic and electronic properties in a much more complicated manner than previously reported. In the range ~ 0.8 -3.5 GPa, the pressure induced metallic state at low temperature is enhanced and the metal-insulator transition (MIT) temperature (T_{MI}) increases with pressure. The MIT coincides with the magnetic transition in this range. Above ~ 3.5 GPa, T_{MI} decreases with pressure increase. At ~ 5 GPa, T_{MI} and magnetic transition temperature start to decouple: T_{MI} drops much faster than the magnetic transition temperature and finally at ~ 6.3 GPa the material becomes insulating and the magnetic transition temperature is almost the same as at ambient pressure.

The samples were prepared by the solid-state reaction method. Stoichiometric amount of Pr_6O_{11} , MnO_2 , and CaCO_3 were mixed, ground and calcined at 1100°C for 70 hours; reground and calcined at 1200°C for 30 hours; the powder was pressed into pellets. Then, the pellets were sintered at 1350°C for 40 hours and annealed by increasing temperature to 1350°C and holding it for 10 hours and then slowly cooling to room temperature at the rate of $1^\circ\text{C}/\text{min}$. All cycles were performed in air. The x-ray diffraction pattern taken at room temperature shows that the samples are in a single crystallographic phase. The structure was refined to Pbnm symmetry using the Rietveld method. The refined lattice parameters are: $a = 5.4301(1) \text{ \AA}$, $b = 5.4676(1) \text{ \AA}$, $c = 7.6751(1) \text{ \AA}$. The sample was also characterized by magnetization measurements (Fig. 1). The magnetization as a function of temperature is consistent with the work of Hwang *et al.*¹⁶ The magnetic moment measured at 5 K is $\sim 2.1 \mu_B/\text{Mn Site}$, approximately equal to that reported by Jiráček *et al.*¹⁴ The details of the high pressure resistivity measurement method were described elsewhere.¹⁷ Because of the lower stability of the measuring system during cooling, the data were only taken in the warming cycle.

Fig. 2 gives the temperature dependence of resistivity at different pressures. At ambient pressure, the material is insulating in the whole temperature range. As re-

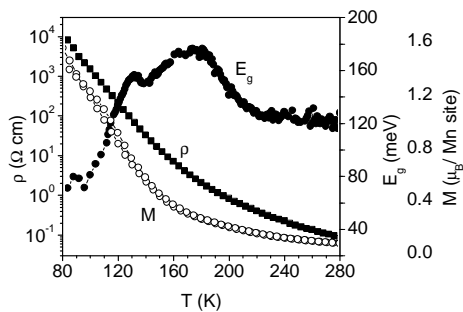


FIG. 1: Temperature dependence of resistivity, magnetization and activation energy of $\text{Pr}_{0.7}\text{Ca}_{0.3}\text{MnO}_3$ at ambient pressure. Magnetization (open circle) was measured in a 10 kOe magnetic field. The resistivity and the activation energy are represented by solid squares and solid circles respectively.

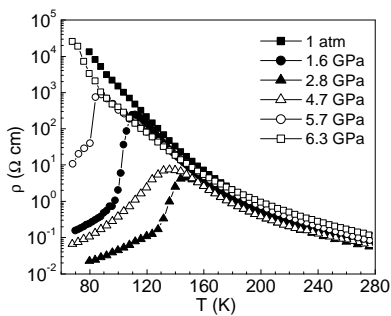


FIG. 2: Temperature dependence of resistivity of $\text{Pr}_{0.7}\text{Ca}_{0.3}\text{MnO}_3$ at different pressures.

ported, pressure induces an insulator to metal transition, which is ascribed to a COI to FMM transition.^{12,16} With pressure increase, the transition temperature T_{MI} (defined as the temperature at the resistivity peak) is shifted up while the resistivity is suppressed at the same time. In the pressure range 3~4 GPa, this trend saturates. At higher pressures, T_{MI} decreases and the resistivity increases. At ~6.3 GPa, the material becomes insulating in the measured temperature range and the resistivity as a function of temperature almost reproduces the case at ambient pressure. The T_{MI} vs. pressure is plotted in Fig. 3. The transition temperature of our sample at low pressure is consistent to that of other authors' polycrystalline samples,¹⁶ but lower than that of single crystals¹² (inset of Fig. 3).

In $\text{Pr}_{1-x}\text{Ca}_x\text{MnO}_3$ ($0.1 \leq x \leq 0.4$), the resistivity displays semiconducting behavior, with the activation energies (E_g) being slightly above 100 meV near room temperature.¹⁴ For $\text{Pr}_{0.7}\text{Ca}_{0.3}\text{MnO}_3$, at ambient pressure, E_g is ~125 meV above ~220 K, then increases upon cooling (Fig. 1). Apparently, the E_g increase corresponds to the charge ordering. On cooling further, E_g decreases to ~80 meV in the range of 100-130 K. It was reported that this compound is phase-separated at low temperature, with the Curie and Néel temperatures of ~115 K and ~130 K, respectively.¹⁴ Hence, by compar-

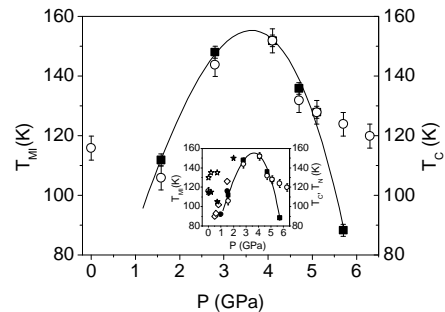


FIG. 3: Pressure induced transition temperatures. The solid squares represent T_{MI} , the solid line is a fit to T_{MI} with a third order polynomial as a guide to the eye; the open circles represent the T_C extracted from the activation energy. (In the inset, the results at low pressures of other authors are displayed for comparison: the solid and open stars are T_C and T_N estimated from the neutron scattering result in ref. 18; The open diamonds represent T_{MI} in the warming cycle estimated from ref. 12, where the sample is single crystal; the solid circles represent T_{MI} in the warming cycle estimated from ref. 15, where the sample is similar to ours.)

ing the temperature dependence of resistivity, magnetization and E_g (Fig. 1), the reduction of E_g can be correlated with the magnetic transition. Yoshizawa *et al.*¹⁸ reported that the CO, AFM and FM transitions appear at different temperature upon cooling below 0.7 GPa, and the CO and AFM components are gradually reduced with pressure increase so that at 2 GPa only FM component is present. From the E_g changes and comparison with the magnetization as a function of temperature and the neutron diffraction results at low pressures,¹⁸ the E_g decrease is associated with the ferromagnetic transition. Consequently, the temperature at which E_g changes fastest with temperature is defined as T_C . The transition temperatures extracted at different pressures are shown in Fig. 3 together with T_{MI} . It is clearly seen that in the measured pressure range of ~1.5-5GPa, T_C and T_{MI} coincide, indicating that pressure destroys the COI state and induces a FMM state at low temperature. But near ambient pressure and above ~5 GPa, the magnetic transition and MIT are decoupled and the material becomes insulating.

In the medium pressure range, at the optimum pressure, both the magnetic transition and metal-insulator transition temperatures reach a maximum. This behavior is similar to that observed in the manganites with a larger bandwidth, in which it can be ascribed to the pressure induced Jahn-Teller distortion and Mn-O-Mn bond angle changes according to the double exchange theory.^{17,19,20}

In the low ($< \sim 0.8$ GPa) and high ($> \sim 5$ GPa) pressure range, the material is more insulating and T_{MI} and T_C are decoupled. In thin films, it was also found that the metal-insulator transition and the magnetic transition decouple.^{21,22} Here, the decoupling may be ascribed to the strong disorder at T_C which can be overcome by the

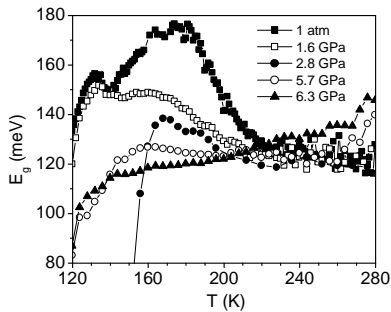


FIG. 4: Activation energy as a function of temperature at different pressures. E_g is calculated as $d \ln(\rho) / d(k_B T)^{-1}$.

magnetization increasing upon cooling so that a metallic state is induced.²¹ The T_{MI} and T_C decoupling in bulk $\text{Pr}_{0.7}\text{Ba}_{0.3}\text{MnO}_3$ is ascribed to the competition between the DE and superexchange (SE) between the Mn-Mn spins.²³ The SE between two neighboring Mn^{3+} can either be FM or AFM depending on the Mn-Mn distance.²⁴ The strength of SE is also a function of the bandwidth W . For the small bandwidth $\text{Pr}_{0.7}\text{Ca}_{0.3}\text{MnO}_3$, at low pressure because of the large lattice distortion, W is small, SE may dominate and the material displays insulating behavior. With pressure increase, due to the local distortion suppression, DE dominates and hence the insulating state is destroyed, yielding a FMM state and T_C increases with pressure. Under pressure, the Mn-Mn distance is monotonically decreased and the local structure distortion of the MnO_6 octahedra may also change as in other manganites.^{17,19,20} When it crosses over an optimum value, SE dominates again.

While pressure changes the electronic and magnetic states, the E_g increase corresponding to charge ordering upon cooling disappears gradually and finally the CO state is completely suppressed so that the activation energy does not change with temperature above the magnetic transition temperature (Fig. 4). The CO phase in the $\text{Pr}_{1-x}\text{Ca}_x\text{MnO}_3$ system is correlated with the lattice distortion and the buckling of the MnO_6 octahedra.¹⁰ At T_{CO} , a transition from dynamic Jahn-Teller distortion to collective static distortion takes place.⁹ Therefore,

the CO state disappearance under pressure (Fig. 4) indicates that the collective static Jahn-Teller distortions are suppressed and that the dynamic distortion possibly dominates at high pressures. From the resistivity and E_g vs. temperature plot at ~ 6.3 GPa, the sample seems to be a FM insulator similar to the $\text{Pr}_{0.75}\text{Ca}_{0.25}\text{MnO}_3$ compound.

In summary, we have measured the electrical resistivity of the small bandwidth manganite $\text{Pr}_{0.7}\text{Ca}_{0.3}\text{MnO}_3$ as a function of temperature and pressure (ambient to ~ 6.5 GPa). It was found that pressure in the range above ~ 2 GPa induces much more complicated changes than in the low pressure range in which pressure only enhances the metallic state. In the studied range, pressure does not always induce an increase in T_C and/or T_{MI} , and the coupling between the magnetic transition and the metal-insulator transition is also tuned by pressure. In this small bandwidth manganite, pressure induces a metallic state in low temperature region. The metal-insulator transition temperature increases with pressure below ~ 3.5 GPa and decreases above ~ 3.5 GPa and the system becomes a ferromagnetic insulator at higher pressures. In the low ($< \sim 0.8$ GPa) and high pressure regions (> 5 GPa), the magnetic and electronic transitions are decoupled. In the medium pressure region, T_C and T_{MI} coincide and change with pressure as in other manganites with large bandwidth. The effects can be ascribed to the pressure tuned competition between DE and SE interactions. In addition to magnetic and electronic states, the charge ordering above magnetic transition temperature is suppressed completely at ~ 3.5 GPa. High pressure measurements of the magnetic structure as well as Raman scattering measurements at different temperatures will shed light on the structural origin of these changes in the magnetic structure with pressure. The complex behavior under pressure enables the assessment of the competition between DE and SE (which both depend on bandwidth and atomic structure) without the need for chemical doping. Hence, this system may become a test-bed for studying highly correlated electron systems.

This work is supported by National Science Foundation Grant DMR-0209243.

¹ Y. Tomioka, A. Asamitsu, H. Kuwahara, Y. Moritomo, and Y. Tokura, Phys. Rev. B **53**, R1689 (1996).
² J. Barratt, M. R. Lee, G. Balakrishnan, and D. M. Paul, Appl. Phys. Lett. **68**, 424 (1996).
³ A. Asamitsu, Y. Tomioka, H. Kuwahara, and Y. Tokura, Nature (London) **388**, 59 (1997).
⁴ V. Kiryukhin, D. Casa, J. P. Hill, B. Keimer, A. Vigliante, Y. Tomioka, and Y. Tokura, Nature (London) **386**, 813 (1997).
⁵ D. E. Cox, P. G. Radaelli, M. Marezio, and S.-W. Cheong, Phys. Rev. B **57**, 3305 (1998).
⁶ M. Hervieu, A. Barnabé, C. Martin, A. Maignan, and

B. Raveau, Phys. Rev. B **60**, R726 (1999).
⁷ K. Miyano, T. Tanaka, Y. Tomioka, and Y. Tokura, Phys. Rev. Lett. **78**, 4257 (1997).
⁸ T. Mori, K. Ogawa, K. Yoshida, K. Miyano, Y. Tomioka, and Y. Tokura, J. Phys. Soc. Jpn. **66**, 3570 (1997).
⁹ V. Dediu, C. Ferdeghini, F. C. Maticcotta, P. Nozar, and G. Ruani, Phys. Rev. Lett. **84**, 4489 (2000).
¹⁰ H. Yoshizawa, H. Kawano, Y. Tomioka, and Y. Tokura, Phys. Rev. B **52**, R13145 (1995).
¹¹ V. Kiryukhin, D. Casa, B. Keimer, J. P. Hill, A. Vigliante, Y. Tomioka, and Y. Tokura, Mat. Res. Soc. Symp. Proc. **494**, 65 (1998).

- ¹² Y. Moritomo, H. Kuwahara, Y. Tomika, and Y. Tokura, *Phys. Rev. B* **55**, 7549 (1997).
- ¹³ J. J. Neumeier, M. F. Hundley, J. D. Thompson, and R. H. Heffner, *Phys. Rev. B* **52**, R7006 (1995).
- ¹⁴ Z. Jiráček, S. Krupička, Z. Šimša, M. Dlouhá, and S. Vratislav, *J. Magn. and Magn. Mat.* **53**, 153 (1985).
- ¹⁵ H. Y. Hwang, T. T. M. Palstra, S.-W. Cheong, and B. Batlogg, *Phys. Rev. B* **52**, 15046 (1995).
- ¹⁶ H. Y. Hwang, S.-W. Cheong, P. G. Radaelli, M. Marezio, and B. Batlogg, *Phys. Rev. Lett.* **75**, 914 (1995).
- ¹⁷ C. Cui, T. A. Tyson, Z. Zhong, J. P. Carlo, and Y. Qin, *Phys. Rev. B* **67**, 104107 (2003).
- ¹⁸ H. Yoshizawa, R. Kajimoto, H. Kawano, Y. Tomioka, and Y. Tokura, *Phys. Rev. B* **55**, 2729 (1997).
- ¹⁹ A. Congeduti, P. Postorino, E. Carmagno, M. Nardone, A. Kumar, and D. D. Sarma, *Phys. Rev. Lett.* **86**, 1251 (2001).
- ²⁰ C. Meneghini, D. Levy, S. Mobilio, M. Ortolani, M. Nuñez-Reguero, A. Kumar, and D. D. Sarma, *Phys. Rev. B* **65**, 012111 (2002).
- ²¹ J. Aarts, S. Freisem, R. Hendrikx, and H. W. Zandbergen, *Appl. Phys. Lett.* **72**, 2975 (1998).
- ²² R. A. Rao, D. Lavric, T. K. Nath, C. B. Eom, L. Wu, and F. Tsui, *J. of Appl. Phys.* **85**, 4794 (1999).
- ²³ A. K. Heilman, Y. Y. Xue, B. Lorenz, B. J. Campbell, J. Cmaidalka, R. L. Meng, Y. S. Wang, and C. W. Chu, *Phys. Rev. B* **65**, 214423 (2002).
- ²⁴ J. B. Goodenough, *Phys. Rev.* **100**, 564 (1955).